AUTHOR QUERY FORM

AIP Publishing	Journal: J. Acoust. Soc. Am. Article Number: 009912JAS	Please provide your responses and any corrections by annotating this PDF and uploading it according to the instructions provided in the proof notification email.

Dear Author,

Below are the queries associated with your article; please answer all of these queries before sending the proof back to AIP.
Please indicate the following:
Figures that are to appear as color online only (i.e., Figs. 1, 2, 3) ____________________________ (this is a free service).
Figures that are to appear as color online and color in print_____________________ (a fee of $325 per figure will apply).

Article checklist: In order to ensure greater accuracy, please check the following and make all necessary corrections before returning your proof.

1. Is the title of your article accurate and spelled correctly?
2. Please check affiliations including spelling, completeness, and correct linking to authors.
3. Did you remember to include acknowledgment of funding, if required, and is it accurate?

Location in article	Query / Remark: click on the Q link to navigate to the appropriate spot in the proof. There, insert your comments as a PDF annotation.
AQ1	Please check that the author names are in the proper order and spelled correctly. Also, please ensure that each author's given and surnames have been correctly identified (given names are highlighted in red and surnames appear in blue).
AQ2	This equation needed to be slashed down per journal style. Please confirm formatting.
AQ3	This in-line equation was slashed down. Please check formatting.
AQ4	Is this (3) a citation to Eq. (3)? Please confirm.
AQ5	Please check inserted Equation citation [Eq. (3)].
AQ6	Please check inserted Equation citation.
AQ7	Please supply page ranges for all articles over 1 page in length unless the 6-digit CID number is given.

Thank you for your assistance.

Generation of vortex waves in non-coaxial cylindrical waveguides

AQ1 Artem S. Pilipchuk,[a)] Alina A. Pilipchuk, and Almas F. Sadreev
Kirensky Institute of Physics, Federal Research Center KSC SB RAS, 660036 Krasnoyarsk, Russia

(Received 10 October 2019; accepted 8 November 2019; published online xx xx xxxx)

A non-coaxial waveguide composed of a cylindrical resonator of radius R and cylindrical waveguides with the radii r_1 and r_2, respectively, is considered. The radii satisfy the inequality $r_1 < r_2 < R$. The conversion from the channel with zero orbital angular momentum (OAM) into the channels with non-zero OAM is achieved by shifting the center lines of the waveguides relative to the center line of the cylindrical resonator. The center lines of input and output waveguides are shifted relative to each other by the angle $\Delta\phi$ in order to twist the output acoustic wave. The conversion efficiency of the input wave with zero OAM into the output wave with non-zero OAM as dependent on the frequency, length of the resonator, and $\Delta\phi$ is considered, and the domains where the efficiency can reach almost 100% are found.
https://doi.org/10.1121/1.5139222

[LZ] Pages: 1–6

I. INTRODUCTION

Vortex waves carrying orbital angular momentum (OAM) have been widely studied in recent years due to many possible applications in medicine, micro-robotics, and biophysics. Distinctive features of such waves are the phase indetermination and null of field magnitude at the propagation axis. Another important property is the helical dislocation of the wavefront: the phase varies as $\exp(im\phi)$, where m is an integer called the winding number or topological charge. Although the existence of such helical dislocations of a wavefront was first predicted by Berry *et al.* (1979) in the wave theory, subsequent studies were mainly continued in optics. It was shown that the dark central spot of optical vortices can confine absorptive or reflective particles (He *et al.*, 1995) or low-index dielectric particles (Gahagan and Swartzlander, 1996) so optical vortices may be used for contactless manipulation of small physical or biological objects—so-called optical tweezers. Since such beams carry OAM, it is possible to induce a rotation of trapped particles (Allen *et al.*, 1992; He *et al.*, 1995).

It was shown using the concept of pseudo momentum that acoustical vortices have the same properties as their optical counterparts (Thomas and Marchiano, 2003) and look very promising. In particular, acoustical tweezers require several orders of magnitude less than that of optical tweezers to apply the same force on particles. Thus, this feature limits spurious heating, which can be crucial for cell or microorganism manipulations. Moreover, acoustical tweezers can be used for particle manipulation in opaque media. All of the above has resulted in significant interest in ways of generating helical waves. The most common setup of acoustic vortices generation is an array of individually addressed transducers providing the appropriate phase and amplitude of the wave front (Hefner and Marston, 1999; Marchiano and Thomas, 2005). However, it requires digital control of each individual pixel of the transducer array, so the resulting device is quite expensive and is not amenable to miniaturization. Gspan *et al.* (2004) demonstrated the optoacoustic generation of a helicoidal ultrasonic beam. They used an absorbing phase plate with a helicoidal profile which was able to generate an ultrasonic wave upon illumination with pulsed laser light due to thermal expansion. There are some techniques based on multi-arm coiling slits (Jiang *et al.*, 2016b; Wang *et al.*, 2016) or an Archimedes' spiral diffraction gratings (Baudoin *et al.*, 2019; Jiménez *et al.*, 2016) which allow generating acoustic vortices with required topological charge determined by the number of spiral arms. Different experimental setups are based on the ferroelectret film glued onto a tangential-helical substrate (Ealo *et al.*, 2011) or a transducer with the phase plate secured to it (Terzi *et al.*, 2017). It is also important to note various setups based on metamaterials. Naify *et al.* (2016) used a leaky-wave antenna to create such vortex waves. Esfahlani *et al.* (2017) proposed the metasurface composed of space-coiled cylindrical unit cells transmitting sound pressure with a controllable phase shift thus transforming an incident plane wave into the desired helical wavefront. Jiang *et al.* (2016a) described an assembled layer consisting of eight fanlike sections of resonators that could transform an incident plane wave into an acoustical vortex in the same way. At last, there is a method based on the inverse filtering technique revised for surface waves (Riaud *et al.*, 2015).

In the present paper, we propose an essentially different method based on a *single* hollow cylindrical acoustic resonator with radius R and two attached cylindrical waveguides with different radii $r_1 < r_2 < R$, as depicted in Fig. 1.

We assume that one of the waveguides, say the output one, can move along the resonator axis to change the resonator length, and rotate around the resonator axis by the angle $\Delta\phi$. It is easy to realize such a system in a realistic acoustic or electromagnetic experiment using the piston-like hollow stem waveguides tightly fit to the interior boundaries of a cylindrical cavity (Lyapina *et al.*, 2015).

[a)]Electronic mail: artem-s-pilipchuk@iph.krasn.ru

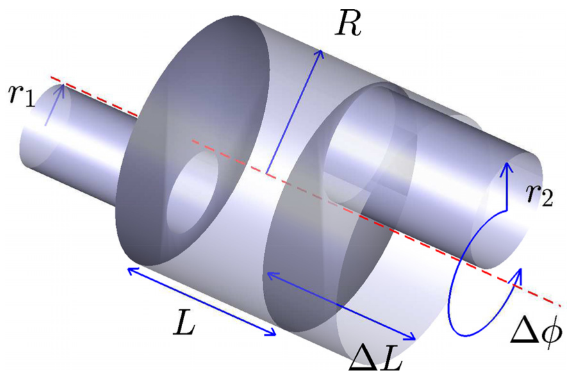

FIG. 1. (Color online) Cylindrical resonator of radius R and variable length L with two attached cylindrical waveguides of different radii r_1 and r_2 where $r_1 < r_2 < R$. The whole waveguide system is non-axisymmetric and the waveguides are misaligned by an azimuthal angle difference $\Delta\phi$. The dashed line is the resonator axis.

In the cylindrical waveguides, propagating modes are classified by azimuthal index p (OAM) and radial index q as shown in Fig. 2, while eigenmodes of a closed cylindrical resonator are specified by azimuthal index m, radial index n, and axial index l. If the waveguides were identical and the whole system was coaxial, there would be transmission from the channel p, q onto the same channel. The angular momentum preserves in the coaxial system, so the input wave with $p=0$ cannot excite the resonator modes with $m \neq 0$, and hence the output wave also has zero OAM. Thus, it is first necessary to break the axial symmetry of the system, for example, by shifting the waveguides' axes relative to the resonator centerline. The next step is to increase the output waveguide radius relative to the radius of the input waveguide, so that the output acoustic wave can propagate not only in the channel with $p=0$, but also in channels with $|p| > 0$, which carry the OAM. And finally, the most important step is to violate the mirror symmetry of the system by rotation of the output waveguide by the angle $\Delta\phi$. As a result, transmittances from the basic channel $p=0$, $q=1$ onto channels $p=1, q=1$ and $p=-1, q=1$ become non-equivalent up to the fact that the conversion onto the channel $p=1, q=1$ substantially exceeds the conversion onto other channels, generating the output wave with angular momentum, i.e., vortical wave. In order to optimize such a generation, we vary two parameters of the system: the resonator length and the rotation angle of output waveguide $\Delta\phi$.

The aim of the present paper is studying the conversion efficiency of the input wave with zero OAM into the output wave with non-zero OAM as dependent on the frequency, the resonator length and $\Delta\phi$.

Neglecting viscosity, we consider acoustic wave transmission described by the linear Helmholtz equation, so there are no flows involved into the process.

II. PROPAGATING MODES IN WAVEGUIDES

In what follows, the model of sound hard boundaries is used, and all the quantities in the model are dimensionless and measured in terms of the input waveguide's radius r_1. The dimensionless frequency is expressed through dimensional one as follows: $\omega = \tilde{\omega} r_1 / s_0$, where $\tilde{\omega}$ is the dimensional frequency and s_0 is the sound velocity in the chosen media. Then, the propagating modes in the Cth cylindrical waveguide are the solutions of the Helmholtz equation and described by Lyapina *et al.* (2018)

$$\psi_{pq}^{(C)}(\rho,\alpha,z) = \psi_{pq}^{(C)}(\rho)\frac{1}{\sqrt{2\pi k_{pq}^{(C)}}}\exp\left(\mathrm{i}p\alpha + \mathrm{i}k_{pq}^{(C)}z\right),$$

$$\psi_{pq}^{(C)}(\rho) = \begin{cases} \dfrac{\sqrt{2}}{r_C J_0(\mu_{0q})} J_0\left(\dfrac{\mu_{0q}\rho}{r_C}\right), & p=0, \\ \sqrt{\dfrac{2}{\mu_{pq}^2 - p^2}}\dfrac{\mu_{pq}}{r_C J_p(\mu_{pq})} J_p\left(\dfrac{\mu_{pq}\rho}{r_C}\right), & p=1,2,3,\ldots, \end{cases} \quad (1)$$

where ρ, α are the polar coordinates in the $x0y$-plane in the waveguides reference system, J is the cylindrical Bessel function of the first kind, μ_{pq} is the qth root of equation $[dJ_p(\mu_{pq}\rho)]/(d\rho)|_{\rho=r_C} = 0$ imposed by the Neumann boundary condition on the walls of sound hard cylindrical waveguide, C enumerates input and output waveguides AQ2

$$k_{pq}^{(C)} = \sqrt{\omega^2 - \mu_{pq}^2 / r_C^2}, \quad (2)$$

$r_1 = 1$. Profiles of the propagating modes $\psi_{pq}(\rho)\cos(p\alpha)$ are depicted in Fig. 2.

The eigenfuctions of the closed cylindrical resonator are given

$$\Psi_{mnl}(r,\phi,z) = \psi_{mn}(r)\sqrt{\frac{1}{2\pi}}\exp\left(\mathrm{i}m\phi\right)\Phi_l(z), \quad (3)$$

where

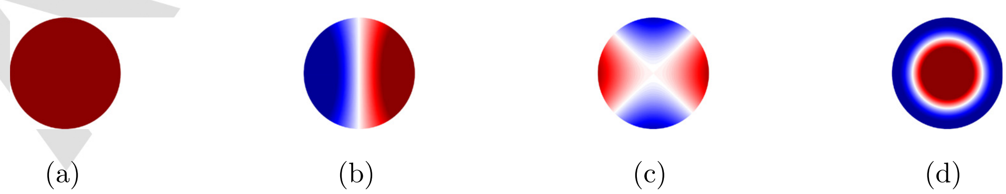

FIG. 2. (Color online) Profiles of propagating modes in the cylindrical waveguide. (a) In channel 1 with cut-off frequency $\omega = 0$ and indices $p=0, q=1$; (b) in channels 2 and 3 with cut-off frequency $\omega = 1.8412$ and indices $p = \pm 1, q=1$; (c) in channels 4 and 5 with cut-off frequency $\omega = 3.0542$ and indices $p = \pm 2, q = 1$; (d) in channel 6 with cut-off frequency $\omega = 3.8317$ and indices $p = \pm 0, q = 2$.

$$\psi_{mn}(r) = \begin{cases} \dfrac{\sqrt{2}}{RJ_0(\mu_{0n})} J_0\left(\dfrac{\mu_{0n} r}{R}\right), & m = 0 \\ \sqrt{\dfrac{2}{\mu_{mn}^2 - m^2}} \dfrac{\mu_{mn}}{RJ_m(\mu_{mn})} J_m\left(\dfrac{\mu_{mn} r}{R}\right), & m = 1, 2, 3, \ldots, \end{cases}$$

$$\Phi_l(z) = \sqrt{\frac{2 - \delta_{l,1}}{L}} \cos\left[\pi(l-1)z/L\right], \tag{4}$$

$l = 1, 2, 3, \ldots,$ ϕ, ρ are the polar coordinates in the $x0y$-plane in the resonator reference system. The corresponding eigenfrequencies are

$$\omega_{mnl}^2 = \left[\frac{\mu_{mn}^2}{R^2} + \frac{\pi^2 (l-1)^2}{L^2}\right], \tag{5}$$

where μ_{mn} is the n-th root of the equation $[dJ_p(\mu_{pq} r)]/$ AQ3 $(dr)|_{r=R} = 0$.

III. CONVERSION FROM THE FIRST CHANNEL INTO HIGHER CHANNELS

Let us inject the wave with zero OAM $p = 0$ and with the frequency obeyed the condition $\mu_{01} < \omega < \mu_{11}$ into the input waveguide with the less radius $r_1 = 1$, i.e., in the first channel according to the classification in Fig. 2. If the radius of the output waveguide r_2 is large enough, i.e., $\mu_{11} > \omega > \mu_{11}/r_2$, the output waveguide supports three propagation channels $p = 0, q = 1$ and $p = \pm 1, q = 1$. In order to allow the channel conversion, we have to break the system axial symmetry. The simplest way is to attach both waveguides in a non-axisymmetric way with center lines of the waveguides shifted by a distance r_0 relative to the center line of the resonator. Moreover, we assume that the waveguide center lines are shifted relative to each other by azimuthal angle $\Delta\phi$ as sketched in Fig. 1. In order to calculate the transmittance, we use the method of the effective non-Hermitian Hamiltonian based on the Feshbach method of projection of the total Hilbert space onto the discrete sub- AQ4 space of the closed resonator eigenmodes [Eq. (3)] (Dittes, 2000; Feshbach, 1958, 1962; Rotter, 1991; Sadreev and Rotter, 2003). We also refer the reader to the papers (Lyapina *et al.*, 2018; Maksimov *et al.*, 2015) where the method was applied to the acoustic transmission through waveguides. The effective non-Hermitian Hamiltonian then takes the following form:

$$\mathbf{H}_{\text{eff}} = \mathbf{H}_{\text{B}} - i \sum_{\text{C=L,R}} \sum_{pq} k_{pq}^{(C)} \mathbf{W}_{pq}^{(C)} \mathbf{W}_{pq}^{(C)^\dagger}, \tag{6}$$

where H_{B} is the Hamiltonian of the closed resonator, $\mathbf{W}_{pq}^{(C)}$ stands for the coupling matrices between the resonator AQ5 eigenmodes mn [Eq. (3)] and the pq eigenmodes of the scat- AQ6 tering channels [Eq. (1)]. For each waveguide, we have the following coupling matrices given by overlapping integrals (Lyapina *et al.*, 2018; Maksimov *et al.*, 2015):

$$\begin{aligned} W_{mnl;pq}^{\text{C}} &= \int_{\Omega_{\text{C}}} \rho d\rho d\alpha \psi_{pq}^{(C)}(\rho, \alpha) \Psi_{mnl}^*(r, \phi, z = z_{\text{C}}) \\ &= \Phi_l(z_{\text{C}}) \int_0^{2\pi} d\alpha \\ &\quad \times \int_0^{r_C} \rho d\rho \psi_{pq}^{(C)}(\rho, \alpha) \psi_{mn}^*(r(\rho, \alpha), \phi(\rho, \alpha)), \end{aligned} \tag{7}$$

where Ω_{C} are interfaces positioned at $z_{\text{C}} = 0, L$. The integration is performed over the circular cross-section of the attached waveguides as shown in Fig. 3. One can link the polar coordinates of the resonator with those of the left waveguide $r\sin\phi = \rho\sin\alpha, r\cos\phi = r_0 + \rho\cos\alpha$. If the radii of the waveguides were equal, the coupling matrix elements for input and output waveguides would be related by only the phase $\Delta\phi$: $W_{mnl;pq}^R(\Delta\phi) = (-1)^{l-1} e^{i(p-m)\Delta\phi} W_{mnl;pq}^L$ (Lyapina *et al.*, 2018). However, in the present case of different waveguides radii, the coupling matrices differ by both phase and strength.

The transmittance of sound waves from the pq propagation channel of the input waveguide through the resonator into the $p'q'$ channel of the output waveguide is given by the equation (Maksimov *et al.*, 2015)

$$t_{pq;p'q'} = 2i\sqrt{k_{pq}^{(L)} k_{pq}^{(R)}} \sum_{mnl} \sum_{m'n'l'} W_{mnl;pq}^{(L)} G_{mnl;m'n'l'} W_{m'n'l';p'q'}^{(R)*}, \tag{8}$$

where

$$\mathbf{G} = \frac{1}{\omega^2 - \mathbf{H}_{\text{eff}}}. \tag{9}$$

The numerical results are presented in Fig. 4. For brevity, we noted $t_{00} = t_{01;01}, t_{01} = t_{01;11}, t_{0-1} = t_{01;-11}$. One can see that the maxima of the transmittance follow the eigenfrequencies of the closed resonator shown by solid lines. This is the feature of three-dimensional systems resulting from the

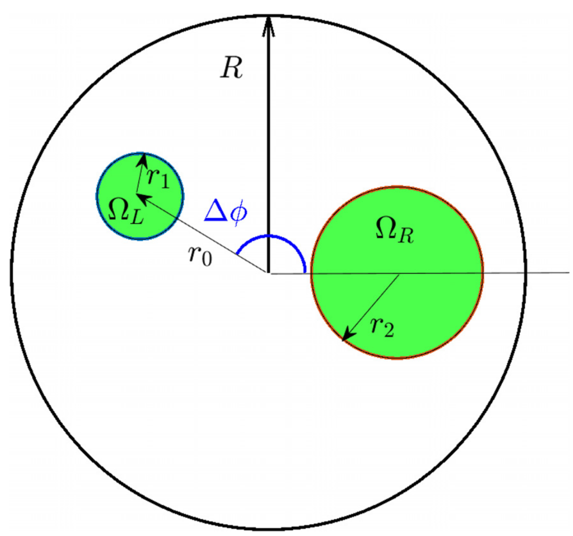

FIG. 3. (Color online) Integration area in the coupling matrix [Eq. (7)] shown by filled areas. r_1 and r_2 are the radii of the attached input and output waveguides. The center line of the waveguides is shifted relative to the center line of the resonator by a distance r_0. Ω_L and Ω_R are integration areas which define the coupling matrix elements [Eq. (7)].

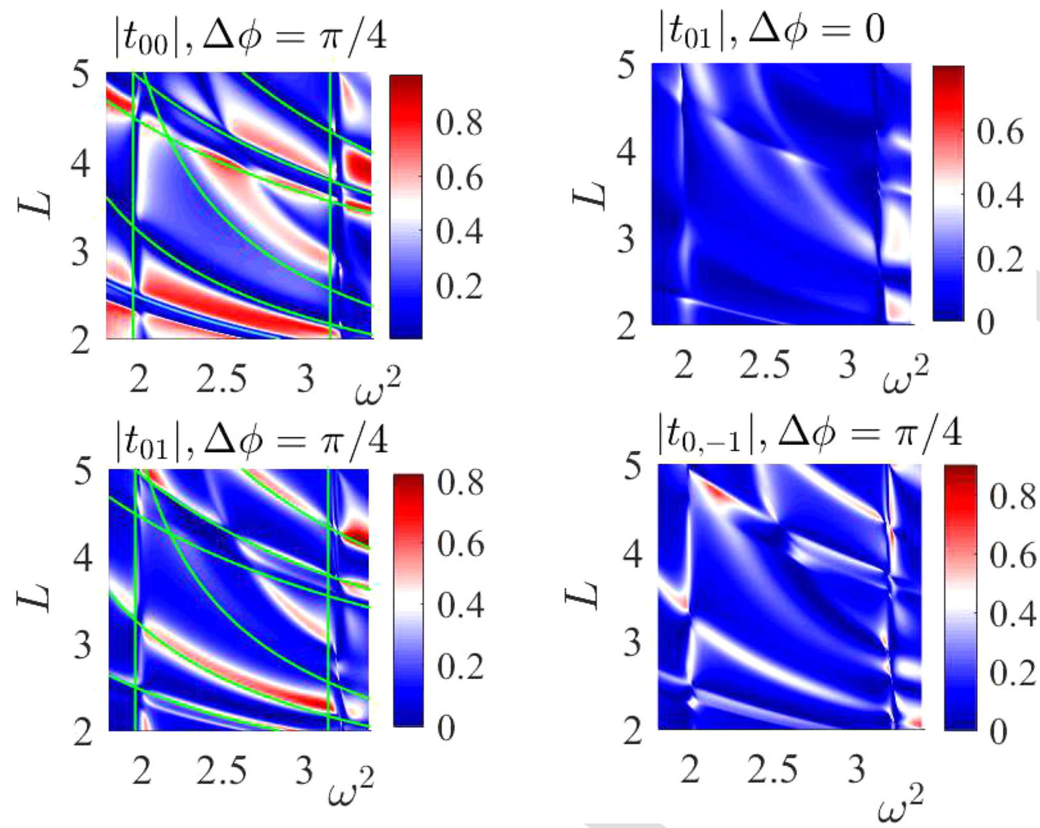

FIG. 4. (Color online) Channel transmittances of a cylindrical resonator with radius $R = 3$ vs frequency ω and length of the resonator L. The center lines of the waveguides with radius $r_1 = 1$ (input) and $r_2 = 1.4$ (output) are shifted relative to the center line of the resonator by distance $r_0 = 1.5$, $\Delta\phi = 0$. Solid lines show the eigenfrequencies of the closed resonator.

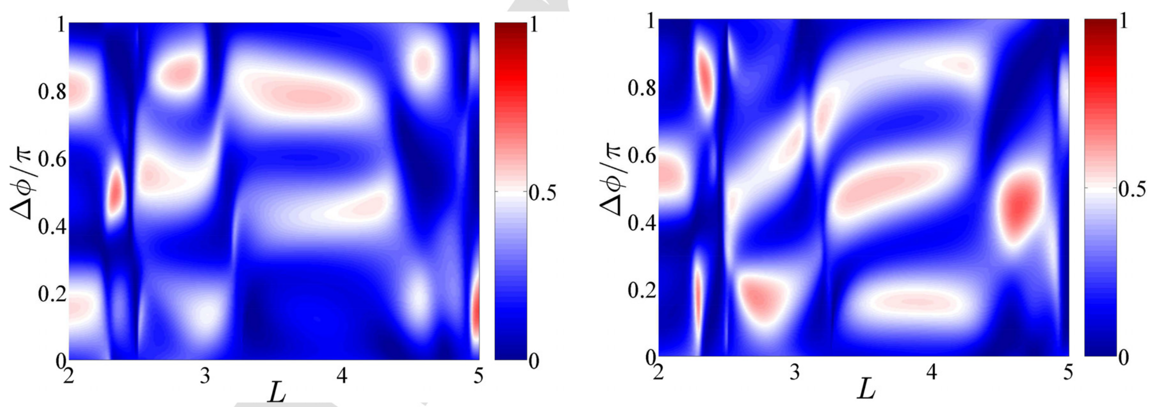

FIG. 5. (Color online) Channel transmittances $|t_{01}|^2$ and $|t_{0-1}|^2$ vs length and for rotation angle $\Delta\phi$ at fixed frequency $\omega^2 = 2$.

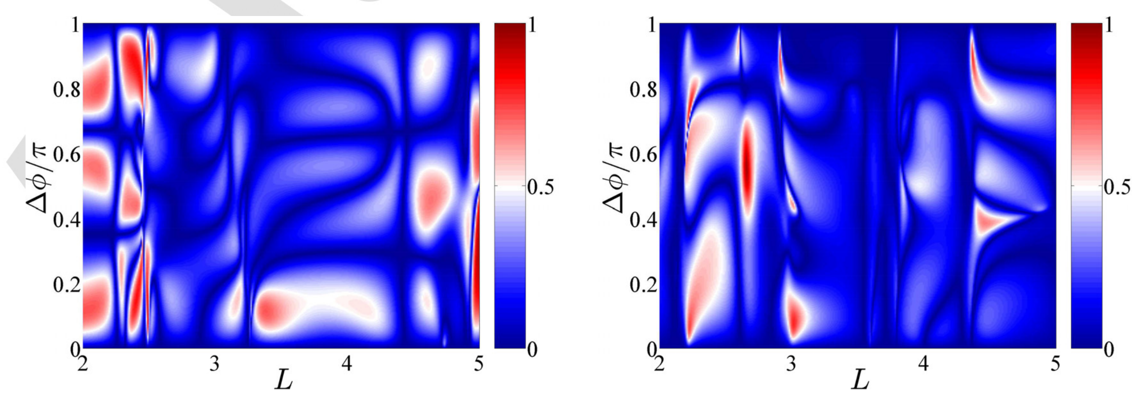

FIG. 6. (Color online) The conversion efficiency [Eq. (10)] vs length of the resonator L and angle of rotation of the input waveguide for (a) $\omega^2 = 2$ and (b) $\omega^2 = 3.1442$.

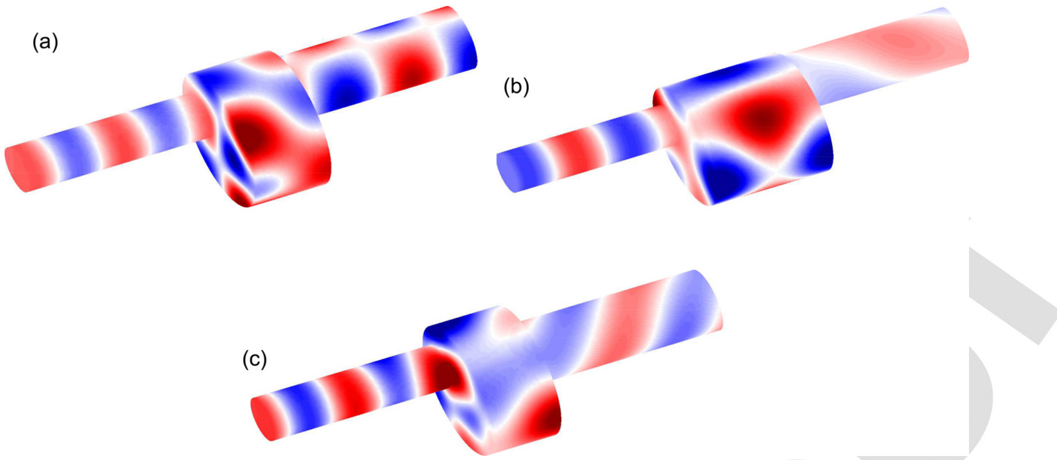

FIG. 7. (Color online) Patterns of scattering functions (the pressure field) at (a) $\omega^2 = 3.3135, L = 2.817, \Delta\phi = 0$, (b) $\omega^2 = 2, L = 4.996, \Delta\phi = \pi/3$, and (c) $\omega^2 = 3.1442, L = 2.6613, \Delta\phi = 0.55\pi$.

weak coupling between the waveguides and the resonator (Lyapina *et al.*, 2018). There is a conversion from the channel $p = 0, q = 1$ onto the channels $p = \pm 1, q = 1$. The transmission coefficients from the first channel with $p = 0$ into channels $p = \pm 1$ are equal to $\Delta\phi = 0, \pi$ to result in the output wave with zero OAM and zero vorticity. However, as soon as $\Delta\phi \neq 0$, transmittances into the channels $\pm m$ become different, i.e., $|t_{01}| \neq |t_{0-1}|$.

IV. TWISTING OF OUTPUT WAVE

The key result is that the transmission from the channel $p = 0, q = 1$ into the channel with the positive OAM $p = 1$ differs from the transmission into the channel with the negative $p = -1$ as soon as $\Delta\phi \neq 0, \pi$ as shown in Fig. 5. Therefore, in order the output wave to be vortical, it is necessary to find the resonator length and angle $\Delta\phi$ at which $t_{00} = 0$ and t_{01} significantly exceed t_{0-1} or vice versa.

We introduce the angular orbital momentum of the output wave as the mean azimuthal index

$$P = \frac{\sum_{p,q} p|t_{01;pq}|^2}{\sum_{p,q} |t_{01;pq}|^2}. \qquad (10)$$

The value P reflects the conversion efficiency of the input wave with zero OAM into the output wave with non-zero OAM. The conversion efficiency [Eq. (10)] versus $\Delta\phi$ and L is shown in Fig. 6 for two selected values of frequency. One can see that for certain resonator lengths and rotation angles, the efficiency can reach almost 100%. Examples of the twisted output wave are shown in Fig. 7.

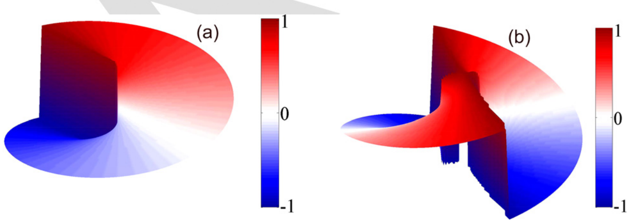

FIG. 8. (Color online) Phase dislocations in terms of π in the output waveguide with radius r_2 for different topological charges: $p = 1$ and $p = 2$.

It is also possible to generate acoustical vortices with the topological charge exceeding one. For that, it is necessary to increase the frequency of the input wave and adjust the system parameters L and $\Delta\phi$. The examples of phase dislocations in the output waveguide are shown in Fig. 8 for two topological charges, one and two.

V. SUMMARY AND DISCUSSION

Generation of vortical acoustic fields by a single cylindrical resonator is based on several basic principles. First of all, the waveguides must be connected to the resonator ends in a non-coaxial way, which allows a wave with zero OAM to excite the resonator modes with nonzero OAM. Next, there must be the conversion from the input channel with $p = 0$ into the output channels with $p \neq 0$, which is achieved by increasing the output waveguide radius relative to the radius of input waveguide. Finally, the waveguides' axes must be shifted relative to each other by a certain angle $\Delta\phi$. This removes the degeneracy of the resonator eigenmodes along with the azimuthal index and gives rise to the rotation of the acoustic field. The numerical calculations show that the conversion efficiency can reach almost 100% for certain resonator length and waveguides' angular shift $\Delta\phi$.

ACKNOWLEDGMENTS

We acknowledge discussions with Dmitrii Maksimov. This work was supported by RFBR Grant No. 18-32-00234.

Allen, L., Beijersbergen, M. W., Spreeuw, R., and Woerdman, J. (**1992**). "Orbital angular momentum of light and the transformation of Laguerre-Gaussian laser modes," Phys. Rev. A **45**(11), 8185. AQ7

Baudoin, M., Gerbedoen, J.-C., Riaud, A., Matar, O. B., Smagin, N., and Thomas, J.-L. (**2019**). "Folding a focalized acoustical vortex on a flat holographic transducer: Miniaturized selective acoustical tweezers," Sci. Adv. **5**(4), eaav1967.

Berry, M. V., Nye, J. F., and Wright, F. (**1979**). "The elliptic umbilic diffraction catastrophe," Philos. Trans. R. Soc. Lond. Ser. A **291**(1382), 453–484.

Dittes, F. (**2000**). "The decay of quantum systems with a small number of open channels," Phys. Rep. **339**(4), 215–316.

Ealo, J. L., Prieto, J. C., and Seco, F. (**2011**). "Airborne ultrasonic vortex generation using flexible ferroelectrets," IEEE Trans. Ultrason. Ferroelectr. Freq. Control **58**(8), 1651–1657.

Esfahlani, H., Lissek, H., and Mosig, J. R. (**2017**). “Generation of acoustic helical wavefronts using metasurfaces,” Phys. Rev. B **95**(2), 024312.

Feshbach, H. (**1958**). “Unified theory of nuclear reactions,” Ann. Phys. **5**(4), 357–390.

Feshbach, H. (**1962**). “A unified theory of nuclear reactions. II,” Ann. Phys. **19**(2), 287–313.

Gahagan, K., and Swartzlander, G. (**1996**). “Optical vortex trapping of particles,” Opt. Lett. **21**(11), 827–829.

Gspan, S., Meyer, A., Bernet, S., and Ritsch-Marte, M. (**2004**). “Optoacoustic generation of a helicoidal ultrasonic beam,” J. Acoust. Soc. Am. **115**(3), 1142–1146.

He, H., Friese, M., Heckenberg, N., and Rubinsztein-Dunlop, H. (**1995**). “Direct observation of transfer of angular momentum to absorptive particles from a laser beam with a phase singularity,” Phys. Rev. Lett. **75**(5), 826.

Hefner, B. T., and Marston, P. L. (**1999**). “An acoustical helicoidal wave transducer with applications for the alignment of ultrasonic and underwater systems,” J. Acoust. Soc. Am. **106**(6), 3313–3316.

Jiang, X., Li, Y., Liang, B., Cheng, J.-C., and Zhang, L. (**2016a**). “Convert acoustic resonances to orbital angular momentum,” Phys. Rev. Lett. **117**(3), 034301.

Jiang, X., Zhao, J., Liu, S.-l., Liang, B., Zou, X.-y., Yang, J., Qiu, C.-W., and Cheng, J.-C. (**2016b**). “Broadband and stable acoustic vortex emitter with multi-arm coiling slits,” Appl. Phys. Lett. **108**(20), 203501.

Jiménez, N., Picó, R., Sánchez-Morcillo, V., Romero-García, V., García-Raffi, L. M., and Staliunas, K. (**2016**). “Formation of high-order acoustic Bessel beams by spiral diffraction gratings,” Phys. Rev. E **94**(5), 053004.

Lyapina, A., Maksimov, D., Pilipchuk, A., and Sadreev, A. (**2015**). “Bound states in the continuum in open acoustic resonators,” J. Fluid Mech. **780**, 370–387.

Lyapina, A., Pilipchuk, A., and Sadreev, A. (**2018**). “Trapped modes in a non-axisymmetric cylindrical waveguide,” J. Sound Vib. **421**, 48–60.

Maksimov, D. N., Sadreev, A. F., Lyapina, A. L., and Pilipchuk, A. S. (**2015**). “Coupled mode theory for acoustic resonators,” Wave Motion **56**, 52–66.

Marchiano, R., and Thomas, J.-L. (**2005**). “Synthesis and analysis of linear and nonlinear acoustical vortices,” Phys. Rev. E **71**(6), 066616.

Naify, C. J., Rohde, C. A., Martin, T. P., Nicholas, M., Guild, M. D., and Orris, G. J. (**2016**). “Generation of topologically diverse acoustic vortex beams using a compact metamaterial aperture,” Appl. Phys. Lett. **108**(22), 223503.

Riaud, A., Thomas, J.-L., Charron, E., Bussonnière, A., Matar, O. B., and Baudoin, M. (**2015**). “Anisotropic swirling surface acoustic waves from inverse filtering for on-chip generation of acoustic vortices,” Phys. Rev. Appl. **4**(3), 034004.

Rotter, I. (**1991**). “A continuum shell model for the open quantum mechanical nuclear system,” Rep. Prog. Phys. **54**(4), 635.

Sadreev, A., and Rotter, I. (**2003**). “S-matrix theory for transmission through billiards in tight-binding approach,” J. Phys. A **36**(45), 11413–11433.

Terzi, M., Tsysar, S., Yuldashev, P., Karzova, M., and Sapozhnikov, O. (**2017**). “Generation of a vortex ultrasonic beam with a phase plate with an angular dependence of the thickness,” Moscow Univ. Phys. Bull. **72**(1), 61–67.

Thomas, J.-L., and Marchiano, R. (**2003**). “Pseudo angular momentum and topological charge conservation for nonlinear acoustical vortices,” Phys. Rev. Lett. **91**(24), 244302.

Wang, T., Ke, M., Li, W., Yang, Q., Qiu, C., and Liu, Z. (**2016**). “Particle manipulation with acoustic vortex beam induced by a brass plate with spiral shape structure,” Appl. Phys. Lett. **109**(12), 123506.